The extra-terrestrial Raman scattering

V. Krishan

Indian Institute of Astrophysics, Bangalore 560 034, India

The diagnostic potential of the Raman scattering of the electro-magnetic radiation has been realized in an all-embracing manner in terrestrial phenomena. Our knowledge of the remote reaches of the universe comes almost entirely from the study of processes responsible for the production and propagation of the electromagnetic radiation. Here, the proposals emphasizing the role of the Raman scattering in diverse astrophysical systems are reviewed with the conclusion that the Raman scattering could turn out to be an extremely versatile tool for cosmic exploration.

The inelastic scattering of electromagnetic radiation by matter is known as Raman scattering. The matter may be in any of the four states: a solid, a liquid, a gas and a plasma. The incident electromagnetic radiation may be monochromatic or a continuum or a combination of the two. The scattered radiation consists of three components: radiation at the incident frequency and two new lines at shifted frequencies, the amount of shift being a characteristic of the scattering medium. Thus, Raman scattering turned out to be a diagnostic tool for studying the structure of molecules and later of crystals. With the realization of lasers, entirely new vistas opened up in the use of Raman effect. A new generation of particle accelerators known as 'beat wave accelerators' have been conceived. These are based on Raman forward scattering, in which two coherent electro-magnetic waves beat to give a Langmuir wave which can accelerate electrons to extremely high energies in a very short time. Novel sources of coherent radiation, the free electron lasers, operate on the principle of Raman back-scattering in which a virtual electro-magnetic wave in the form of a spatially periodic magnetic field is scattered by a Langmuir wave. The frequency of the scattered radiation is $\sim\gamma^2$ times the frequency of the virtual electromagnetic wave where γ is the Lorentz factor of electrons.

The universality of the Raman effect, as emphasized by the discoverer himself seems more true today than ever before. The study of Raman effect has been extended from molecules to magnetohydrodynamics; from rotation-vibration spectra to waves Alfvenic and Langmuir; in laboratories terrestrial to celestial. This paper is an inventory of the work done on Raman scattering in various astrophysical situations. In a few of these, the diagnostic potential of Raman scattering has been recognized and in the others, it awaits. The literature cited is only a lead to that which is and to that, which will be ours to see.

Molecular Raman scattering

Molecules in a gas may or may not have permanent electric dipole moments. If they do, the dipole moments are directed in a random fashion and the net dipole moment is zero.

When an electromagnetic wave impinges upon a molecule, it disturbs the distribution of charge around the molecule, thereby inducing an electric dipole moment. In addition the electric dipole moments of the molecules tend to align themselves with the incident electric field. The system acquires a net dipole moment. The radiation produced by these induced moments is then seen as the scattered radiation. The polarization P which is the total dipole moment per unit volume is therefore a function of the impinging electric field E and can be written as a power series in E as:

$$P_i = \sum_j \alpha_{ij} E_j + \sum_{j,k} \beta_{ijk} E_j E_k + \cdots, \tag{1}$$

where the ccefficients α, β are the electric susceptibilities which are in general functions of the frequencies of various electric fields acting on the molecules. The electric susceptibilities lead to the phenomena of refraction and harmonic generation. The induced dipole moment P of the molecules in the linear limit can be expressed as

$$P = \alpha E_0 \cos 2\pi \nu_0 t, \tag{2}$$

where α represents the polarizability and E_0 the amplitude of the electric field oscillating with frequency ν_0. The polarizability α is a function of the configuration of the molecule and varies with the vibrational or other motions of the nuclei. For atoms in a periodic state of motion of frequency ν_m, the polarizability can be written as

$$\alpha = \alpha_0 + \alpha_1 \cos 2\pi (\nu_m t + \varphi), \tag{3}$$

where α_0 is the polarizability in the equilibrium configuration, α_1 is the amplitude of the oscillating polarizability and φ is an arbitrary phase. Thus, from

equation (2), we find

$$P=\alpha E_0 \cos(2\pi\nu_0 t)+\alpha_1 E_0 \cos(2\pi\nu_0 t)\cos 2\pi(\nu_m t+\varphi).$$

The induced dipole moment has three components oscillating at ν_0, $(\nu_0+\nu_m)$ and $\nu_0-\nu_m$ and gives rise to radiation at these three frequencies corresponding to Rayleigh line at ν_0 and Stokes–Raman and anti-stokes-Raman lines at $(\nu_0-\nu_m)$ and $(\nu_0+\nu_m)$ respectively. Thus, we see that the origin of the Raman lines lies in the temporal changes of the polarizability[1] caused due to molecular motion in which ν_m may be associated with a rotational or a vibrational mode. Though the power emitted by an oscillating dipole can be calculated using the classical electromagnetic theory, the diagnostic capabilities of the Raman scattering are revealed within the framework of the quantum theory. From the quantum description of the Raman scattering one learns that this is a three-level process in which a molecule in the initial state of energy E_i absorbs the incident photon of frequency ν_i and attains an intermediate state $|E_i+h\nu_i\rangle$ which is not a true bound state. The molecule reaches the final state, $|f\rangle$, a true bound state with the emission of a photon of frequency ν_f such that $E_i+h\nu_i=E_f+h\nu_f$. In contrast, in the resonant line scattering, the intermediate state $|E_i+h\nu_i\rangle$ corresponds to a true bound state of the scattering molecule. Thus the Raman scattering permits a wider choice of the incident radiation field and enhances its observability by transferring it into an observationally more accessible region of the spectrum.

Raman scattering in planetary atmospheres

The molecular hydrogen is the major constituent of the atmospheres of the major planets. The absence of a permanent electric dipole moment in H_2 makes its detection impossible through ordinary rotation-vibration spectra. However H_2 does possess a permanent quadrupole moment and therefore the corresponding, though weak rotation–vibration spectrum. Herzburg[2] was the first to suggest the possible detection of H_2 and N_2 by observing their quadrupole transitions in planetary and stellar atmospheres through Raman scattering. Raman scattering[3-5] by H_2 can reduce the ultraviolet albedo of the planets as well as fill in and produce ghosts of the solar absorption lines. The observations in Uranus, of the Raman ghosts of Fraunhofer and their filling in provide direct evidence for the Raman scattering. Cochran and Trafton[3] developed detailed models of Raman scattering in inhomogeneous planetary atmospheres to explain the blue and ultraviolet extinction; filling in of the cores of solar lines and the production of Raman-shifted ghosts of the Fraunhofter spectrum, particularly of the Ca II H and K lines. The cross-section for Raman scattering by hydrocarbons has also been discussed in these papers. Wagener and Caldwell[4] have shown that the measured geometric albedos of the planets Uranus and Neptune between 2100 and 3350 Å compare very well with those calculated in a Rayleigh–Raman scattering atmosphere. Yelle *et al.*[5] analysed the solar reflection spectrum obtained by the voyager ultraviolet spectrometer at wavelengths between 1200 and 1700 Å and pointed out the necessity of including Raman scattering.

Such studies lead to a better understanding of the temperature and pressure structure as well as the infrared spectra of the planetary atmospheres.

Raman scattering in symbiotic stars

Symbiotic systems are binary stars consisting of a cool mass losing giant and a hot ionizing radiation source. Strong and broad emission lines at λ6830 and λ7088 have been observed in about half of the known symbiotic stars. There exists a strong correlation between the intensities and the profiles of the two emission features. The band at λ6830 is observed only in those symbiotics which produce high excitation lines like Ne V and Fe VII. Schmid suggested that these emission features are produced through the Raman scattering of OVI lines λ1032 and λ1038 originating in the inner HII region by the neutral hydrogen in the environs of the cooler star[6-9].

A hydrogen atom in the state 1S absorbs a photon at λ1032 to reach a metastable state just below the 3P level from which it falls to the stable state 2S after the emission of a photon at λ6830. The emission at λ7088 also takes place via the same route. The scattered radiation (*f*) mimics the spectral shift or width of the incident radiation (i) i.e. $\Delta\nu_i=\Delta\nu_f$ or in terms of wavelengths

$$(\Delta\lambda_f/\lambda_f)=(\lambda_f/\lambda_i)\,(\Delta\lambda_i/\lambda_i).$$

Thus, in the case of Raman scattering, where $\lambda_f>\lambda_i$, the scattered line is a better candidate for the determination of the linewidths and shifts. The Raman scattering can, therefore result in a rather broadened line profile which may be erroneously attributed entirely to micro- and macroturbulence. The polarization measurements[10] of the emission features at λ6830 and λ7088 are a further pointer to their generation by a scattering mechanism. Thus, Raman scattering as a probable excitation mechanism is rich with diagnostic potentialities as it bears the signatures of (i) the source of the incident radiation and (ii) the geometry, composition, temperature and time variability of the scattering region and hence offers the essentials for building the models of symbiotic stars.

Raman scattering in the interstellar medium

Atomic hydrogen in the galaxy is found to be distributed in the manner of the blue stars. The inferences are that either the gas-rich sites are the birthplaces of the stars or that the blue stars are responsible for the dissociation of the generally abundant molecular hydrogen into atomic hydrogen. Prof. M. Krook (of Gold[11]) suggested that the Lyman α from the blue stars could undergo Raman scattering on molecular hydrogen. The emission features characteristic of the molecular gas should then appear on the redward of the Lyman α. The detection of these features in the ultraviolet spectrum of the nebular region of the blue stars could then provide a handle on the abundance and other properties of the gas. The inherent weakness of the Raman effect could be offset by the large fluxes of Lyman α resulting from the short mean free path of the Lyman α photons in the atomic hydrogen region[12]. Radhakrishnan *et al.*[13] proposed stimulated Raman scattering as an explanation for the exceptionally wide spectrum of H_2O sources since Doppler shifts turned out to be inadequate[13].

Raman scattering in high energy sources

Hard X-ray and γ-ray burst sources are believed to be strongly magnetized. Therefore, emission features at the electron cyclotron frequency should be detected in these sources. Such a feature has been detected in Her X-1. Direct and inverse Compton scattering processes are held responsible for the shape of the emerging spectrum. Several suggestions for the photon sources include the thermal synchrotron and higher order photon diffusion processes. In the limit that the electron cyclotron radius approaches the Compton wavelength, the electron motion must be quantized with its energy defined by discrete Landau levels. Miska and Miska[14] envisage an electron–photon scattering in which the electron is pushed to a higher Landau level from which it may relax to a lower Landau level by the emission of a photon. This is Raman scattering. Its inclusion as a radiative transfer mechanism is emphasized.

Raman scattering in Seyfert galaxies

Nussbaumer' *et al.*, nave proposed Raman scattering for the generation of the hitherto unidentified emission lines at λ1519 and λ1594 observed in some of the Seyfert galaxies. Here, a HeII Lyman β photon near λ256 is absorbed by He^+ which then emits the scattered photon near λ1640. A list of the probable incident radiation lines near λ256 and the scattering ions along with the transitions leading to the scattered radiation in the range λ1300 to λ2000 is given[7] while reminding us of the accessibility of this spectral region through the international ultraviolet Explorer and the Hubble space telescope. So, more identifications may be in the offing.

Stimulated Raman scattering in plasmas

There are three ways by which the scattering of radiation in a plasma can occur: (i) the stimulated Raman scattering (SRS), where a strong electromagnetic wave is scattered off a weakly damped electron plasma wave ($k_l << k_D$), (ii) the stimulated Compton scattering (SCS), where a strong electromagnetic wave is scattered off a highly damped electron-plasma wave ($k \geq k_D$) and (iii) the Compton scattering (CS) where the electromagnetic radiation is scattered by single electrons (ε, p) (Figure 1). Here k_D is the Debye wave vector and k_l is the wave vector of the electron-plasma wave.

STIMULATED RAMAN SCATTERING $(k_l \ll k_D)$

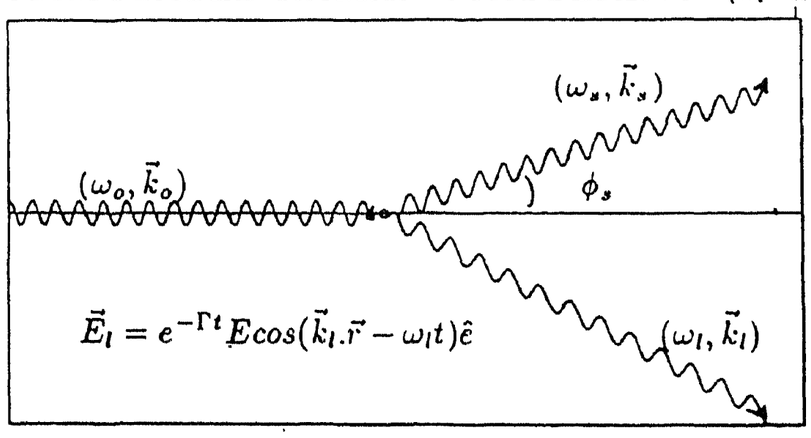

$\vec{E}_l$ is the electric field of a weakly damped electron plasma wave.

STIMULATED COMPTON SCATTERING $(k_l \geq k_D)$

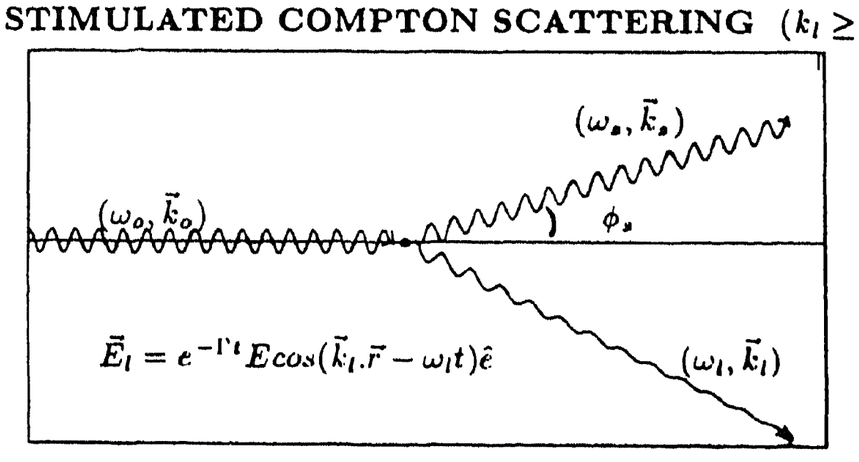

$\vec{E}_l$ is the electric field of a highly damped electron plasma wave.

INVERSE COMPTON SCATTERING

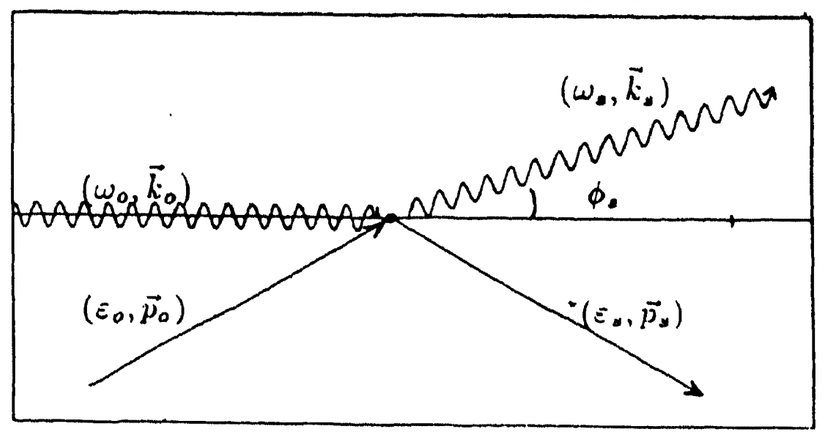

Figure 1. The scattering of radiation $(\omega_0, \vec{k}_0)$ in a plasma.

The stimulated Raman scattering[15] is the resonant decay of an incident photon (ω_0, k_0) into a scattered photon (ω_s, k_s) and an electron-plasma wave (ω_l, k_l) such that

$$\omega_0 = \omega_s + \omega_l,$$

$$\vec{k}_0 = \vec{k}_s + \vec{k}_l,$$

where ω_0 and ω_s satisfy the dispersion relation: $\omega_0^2 = \omega_{pe}^2 + k_0^2 c^2$ and ω_{pe} is the electron plasma frequency. Since the minimum value of ω_0 is ω_{pe}, the Raman process can occur only for $\omega_0 \geq 2\omega_{pe}$ or for electron density $n \leq n_{cr}/4$, where $4\pi n_{cr} e^2/m = \omega_0^2$. In this process, it is evident that the fraction of the energy transferred to the electron-plasma wave is (ω_l/ω_0) and this is the energy that is available for heating the plasma electrons by the damping of the electron-plasma wave. The stimulated Raman scattering takes place in the manner of an instability. When an electromagnetic wave of amplitude E_0 propagates through a plasma with rippled density $(n_0 + \delta n)$ profile created by the electron plasma wave, a transverse current $\delta J = -e\delta n \vec{V}_0$ is generated where $\vec{V}_0 = e\vec{E}_0/m\omega_0$ is the quiver velocity of the electrons. Under proper conditions of phase matching, the transverse current $\delta\vec{J}$ produces a scattered electromagnetic wave $\vec{E}_s$ which interferes with the incident wave to produce a variable wave pressure $\Delta(\vec{E}_0 \cdot \vec{E}_s/4\pi)$. The corresponding force known as the ponderomotive force pushes the plasma from a high pressure region to a low pressure region and vice versa and the consequent generation of a density ripple occurs. Thus, the feedback loop is completed and the instability is excited. The multifarious activities of the instability in the ionospheric as well as the quasar plasmas are discussed in the following sections:

Stimulated Raman scattering in the ionosphere

The ionosphere has been irradiated with high frequency radio radiation from several ionospheric modification facilities situated all over the world[16]. The propagation of the intense radio waves through the ionosphere plasma gives rise to the phenomenon of parametric instabilities, the stimulated Raman scattering (SRS) being one of them. The SRS offers an unambiguous interpretation of the emission feature observed[17] at the half harmonic $(\omega_0/2)$ of the incident radiation at the frequency ω_0. The SRS takes place at a plasma level such that $\omega_0 \simeq 2\omega_p$ (also known as the quarter critical region) since here the electron density $n = n_c/4$ where $\omega_0^2 = 4\pi n_c e^2/m$). The diagnostic value of SRS lies in the fact that the scattered wave is impregnated with the information on the electron density, temperature and the inhomogeneities in them.

Stimulated Raman scattering in quasar plasmas

The importance of plasma processes in the generation of the quasar continuum radiation and its interaction with the surrounding plasma is pointed out, particularly emphasizing their coherent nature, due to which the scattering and absorption rates are enhanced sometimes by several orders of magnitude over the ones obtained from single particle processes.

The continuum emission

The continuum emission of a quasar is in the form of a power law $F_\nu \alpha \nu^{-\alpha}$, consisting of several components; in the low frequency ($\nu \leq 1$ GHz) radio region, $\alpha \simeq 0.1$; in the X-ray region $\alpha \leq 0.7$. The entire spectrum when fitted with an average value of $\alpha = 1$ shows bends in the radio, bumps in the blue and distinct variations in the hard X-ray and γ-ray regions. The continuum originates very near the black hole and then interacts with the surrounding plasma, which as a result exhibits phases of diverse temperatures and densities.

The earlier models of the continuum emission include synchrotron process for the radio radiation, which is upshifted to optical and X-rays by the single particle Compton scattering.

The role of stimulated scattering processes has been investigated in an endeavour to model the generation of nonthermal quasar continuum. Preliminary attempts[18–20] to reproduce almost the entire spectrum of the quasar 3C273 by a suitable combination of SRS and SCS appear quite promising. In particular, the specific features like bumps in the blue and red regions could be interpreted as a change of emission process from SRS to SCS (Figure 2). In the process of reproducing the

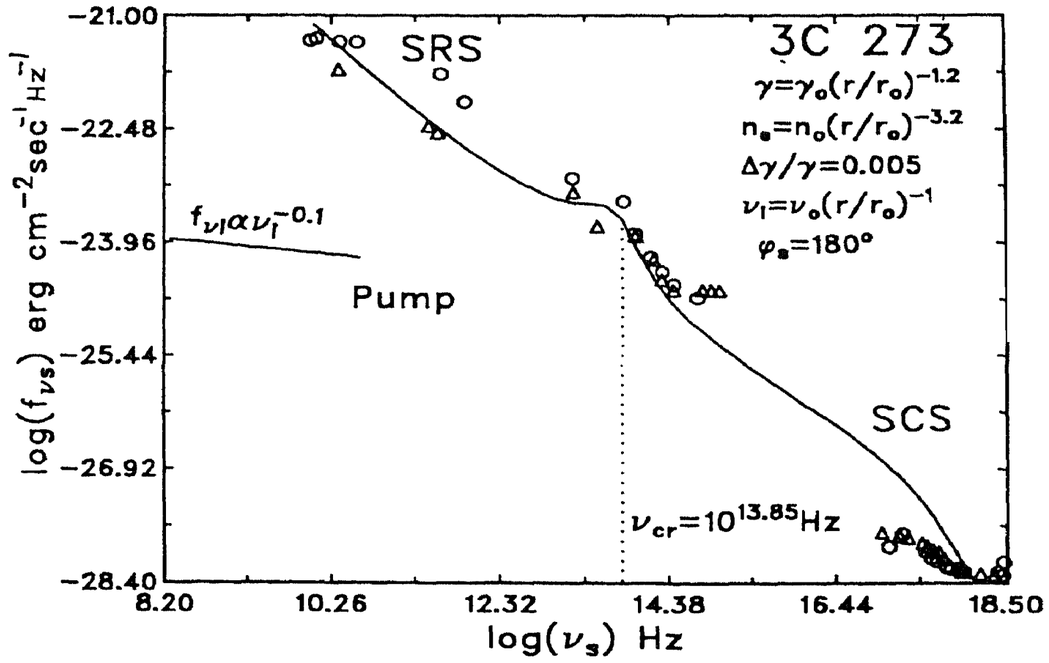

Figure 2. Spectrum of the quasar 3C 273. The solid lines represent the calculated spectrum and the spectrum of the pump wave. The observed points, O (1984 February) and Δ (1986 February) by Courvoisier *et al.* (*Astron. Astrophys.*, 1987, **176**, 197–209), are also plotted. The constants are: $\gamma_0 = 3 \times 10^3$, $n_0 = 9.24 \times 10^{17}$ cm^{-3}, $\nu_0 = 4 \times 10^{10}$ Hz.

observed spectrum, one is also able to derive the spatial variations of the plasma parameters in the emission region. That these variations are compatible with the geometry and stability of the accretion flows need to be scrutinized.

If the electron energy is converted into radiation via the extremely fast processes of SRS and SCS, then it must also be replenished at a comparable rate for the sustained emission from the quasars. The Raman forward scattering[19,21] in which the electron-plasma waves produced by the beating of the cyclotron lines provide the necessary electric field for accelerating the electrons, could be one such process. Several issues related to the efficiency of these processes in the rather inhomogeneous and variable environment of a quasar need to be investigated in depth.

Anomalous absorption and scattering of the quasar radiation

The electron densities of the thermal plasma in the environs of a quasar are such that the corresponding electron plasma frequencies lie in the range of radio frequencies. This opens up several avenues by which the radio radiation can be absorbed in the thermal plasma by processes more efficient than the collisional. Again, through the processes of the parametric decay instability and the stimulated Raman and Compton scattering followed by the damping of the electron plasma and the ion acoustic waves, the plasma can be heated to much higher temperatures in much shorter times. The plasma temperature is one of the most important factors in the emission of continuum and line radiation and is also responsible for the inhomogeneous distribution of the gas[22].

The occurrence of superluminal motion in extragalactic radio sources is believed to be quite common. Among others, the geometrical scattering of radio radiation can also cause superluminal expansion and or motion and a halo formation. The apparent motion of the source is interpreted[23] to be nothing but the Raman scattered radiation of a rotating source at increasing scattering angles. The advantages of this coherent scattering process are the preservation of the flux and its spectral characteristics after the scattering, provided the plasma parameters are chosen appropriately.

Several high energy sources like quasars and pulsars show extremely rapidly varying polarization characteristics of their radiation. For example, some pulsars show a flip of a right-handed circular polarization to a left-handed circular polarization within a pulse period. Since coherent processes have the shortest time scales and scattering always causes polarization changes, the Raman scattering appears to be an attractive mechanism for rapid polarization variability. It appears possible to change the sense of rotation as well as the inclination of the polarization ellipsoid through the stimulated Raman scattering processes[24].

Conclusion

The diagnostic potential of the Raman scattering, whether in gases, liquids, solids or plasmas has always been recognized and put to a good use. Its play in the near and the far reaches of the universe has also been acknowledged to some extent. It may not be premature to say that some of the difficulties in understanding the complex spectra of the distant objects like quasars, specifically the red shift anomalies of apparently neighbourly sources may be resolved by including Raman scattering in the scheme of things. The stimulated Raman scattering in plasmas could turn out to be a strong candidate for the generation of coherent radiation in high energy sources. The ionospheric detection of the stimulated Raman scattering should be motivation enough to look for it elsewhere in the universe.

1. Anderson, A., *The Raman Effect*, vol. 1, Macel Dekker, New York, 1971.
2. Herzburg, G., *Astrophys. J.*, 1938, **87**, 428–437.
3. Cochran, W. D. and Trafton, L. M., *Astrophys. J.*, 1978, **219**, 756–762.
4. Wagner, R. and Caldwell, J., *Icarus*, 1986, **67**, 281–288.
5. Yelle, R. V., McConnell, J. C. and Strobel, D. F., *Icarus*, 1989, **77**, 439–456.
6. Schmid, H. M., *Astron. Astrophys.*, 1989, **211**, L31–34.
7. Nussbaumer, H., Schmid, H. M. and Vogal, M., *Astron. Astrophys.*, 1989, **211**, L27–30.
8. Schmid, H. M., *Astron. Astrophys.*, 1992, **254**, 224–240.
9. Isliker, H., Nussbamur, H. and Vogal, M., *Astron. Astrophys.*, 1989, **219**, 271–275.
10. Schild, H. and Schmid, H. M., *Curr. Sci.*, 1992, **63**, 537–539.
11. Gold, T., *Mem. Cociété Royal des Sciences de Liege Series*, 1961, No. 5, **4**, 476–484.
12. Dalgarno, A. and Williams, D. A., *Mon. Not. R. Astron. Soc.*, 1962, **124**, 313–319.
13. Radhakrishnan, V., Goss, W. M. and Bhandari, R., *Pramana*, 1975, **5**, 49–58.
14. Miska, E. M. and Miska, D., *Astrophys. J.*, 1987, **317**, 282–289.
15. Liu, C. S. and Kaw, P. K., *Adv. Plasma Phys.*, 1976, **6**, 83–119.
16. Thide, B., *Phys. Scr.*, 1990, **T30**, 170–180.
17. Derblom, H. *et al.*, *J. Geophys. Res.*, 1989, **94**, 1011–1021.
18. Krishan, V., *Astrophys. Lett.*, 1983, **23**, 133–138.
19. Krishan, V. and Wiita, P. J., *Mon. Not. R. Astron. Soc.*, 1990, **246**, 597–607.
20. Gangadhara, R. T. and Krishan, V., *Mon. Not. R. Astr. Soc.*, 1992, **256**, 111–120.
21. Krishan, V., *Astrophys. Space Sci.*, 1985, **115**, 119–126.
22. Krishan, V., *Mon. Not. R. Astr. Soc.*, 1988, **230**, 183–187.
23. Krishan, V., *J. Astrophys. Astron.*, 1988, **9**, 231–236.
24. Krishan, V. and Gangadhara, R. T., Proceedings of International Conference on Plasma Physics, Innsbruck, 1992, pp. 1671–1673.

Received 18 November 1992; accepted 5 January 1993